ELECTRO-OPTICAL OPTIMIZATION OF C-SI THIN SOLAR CELLS PATTERNED BY PHOTONIC CRYSTALS

F. Mandorlo[1], R. Peretti[2], L. Lalouat[2], G. Gomard[2], L.C. Marion[1], X. Meng[2], A. Fave[1], C. Seassal[2], E. Drouard[2]

University of Lyon, Lyon Institute of Nanotechnology (INL) UMR CNRS 5270
[1] INSA de Lyon, Villeurbanne, F-69621, FRANCE
[2] Ecole Centrale de Lyon, Ecully, F-69134, FRANCE

Abstract: Using Photonic Crystals (PC) to pattern the top surface of thin film solar cells aims at increasing absorption in the red part of the solar spectrum. In this conference, we explain that a PC also introduces new optical properties for high energy photons since they can be channeled through the holes of the PC itself. Then, optical intensity at the corresponding wavelength is mainly located into the air (or cladding media), leading to a lower effective absorbing constant compared to the bulk material. In other words, these photons can be absorbed further from a carrier collector located at the surface, where carrier recombinations are elevated due to a high doping level. Unfortunately, surface recombinations are even more critical since the residual absorption of the channeled photons is mainly located on the lateral surface of the holes.
In this communication, we focus on the influence of the junction location, the shape of the top contact doping profile (conformal or not) and on the influence of the surface passivation to obtain a robust devices.

Keywords: Thin Film Solar Cell, Photoelectric Properties, Photonic crystal.

INTRODUCTION

In order to reduce the cost of solar cells, one of the trends consists in using thin film c-Si solar cells. To compensate their lower volume of active absorbing material, different technologies are used to increase the interaction of photons in the device [1], [2].

Patterning the surface with a 2D photonic crystal (PC) can increase the photons lifetime in the absorber when the latter is too thin (typically $< 5\ \mu m$) to absorb low energy photons [3], [4], [5]. The height of the patterns must be high enough to ensure a sufficient light trapping, but increasing their height also increases the amount of surfaces where carrier can recombine. Consequently, performances of patterned thin solar cells are more sensitive to the passivation scheme than flat ones.

The two following parts depict the challenges to collect light efficiently in c-Si thin film solar cells with:

- optical constraints: photogerated carriers must be located where electrical collection is efficient, far from recombinating surfaces and preferentially in low doped volumes.
- electrical constraints: the increased amount of surfaces to be passivated due to the patterning must not affect too much the carrier collection.

1. OPTICAL OPTIMIZATION AND CHANNELING

1.1. Main optical regimes of PC-patterned solar cells

The influence of patterning on the absorbed optical energy is depicted in figure 1 for a non optimized set of parameters. The absorption spectrum can be divided into 3 main areas [6] where the patterning acts as:

- an anti-reflection system ($\lambda_0 \leq 500\,nm$), leading to a significant increase of the absorption in the absorber;
- a Fabry Perot cavity ($500\,nm \leq \lambda_0 \leq 650\,nm$), since photons reflect on the rear surface of the solar cell and create interferences in the absorber;
- a PC ($\lambda_0 \geq 650\ nm$) where photons lifetimes in the absorber is increased compared to a bulk device, what ever the wavelength.

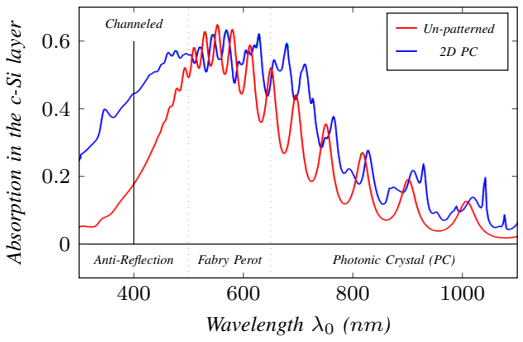

Figure 1: Influence of a 2D PC patterning on the absorption spectrum for a thin c-Si absorber

In order to obtain an efficient cell, the aim of the patterning mainly consists in increasing the photogeneration rate in the absorber.

1.2. Channeling at short wavelength

For particular wavelengths in the anti-reflection area (fig. 1), the map of the electric field looks like figure 2.

3D FDTD applied on a simple structure made of a single a-Si:H layer with a 2D square lattice of cylindrical holes demonstrates that the energy of such optical signals is mainly located in the hole itself leading to an effective attenuation in the vertical direction that is lower than in bulk absorber (fig. 3).

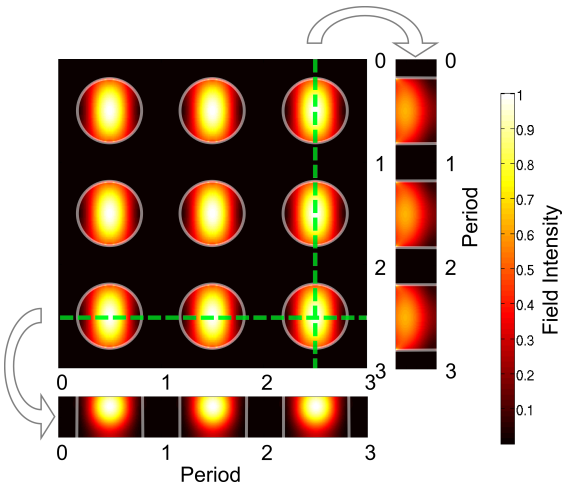

Figure 2: Top view of the electric field in a channeled regime into a thin membrane for a spatial period around 500 nm.

For penetration depth higher than 20 nm, the effective medium theory (EMT) also over estimates the absorption compared to exact computation (3D FDTD in fig. 3).

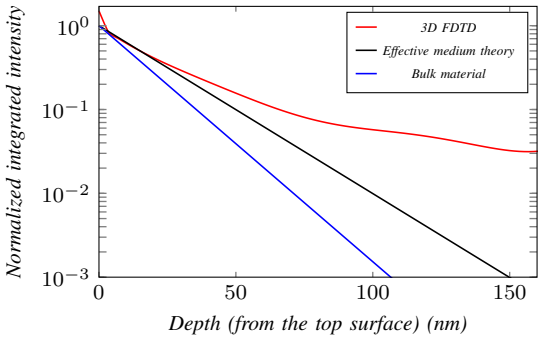

Figure 3: Absorption of a channeled signal

Consequently, short wavelength photons can also benefit from the PC patterning since their absorption in the solar cell can be extended far away from the top surface.

1.3. Optimization of the photogeneration rate

Figure 4 depicts the c-Si simulated device by 3D FDTD where an ITO layer acts as an anti reflective coating layer and helps carrier collection to compensate the poor lateral conductivity of a a-Si layer that collects electrons and passivates the absorber (c-Si) [7].

In order to consider carriers that can be easily collected, the optimization of 3D FDTD [8] aims in maximizing the absorption in the c-Si (both in the absorber and in the holes collector). This condition leads to underestimate the short circuit current J_{sc} since few carriers can be collected in the amorphous silicon constituting the electrons collector. Then, we obtain a 100 nm height pattern with a filling factor of 55 %.

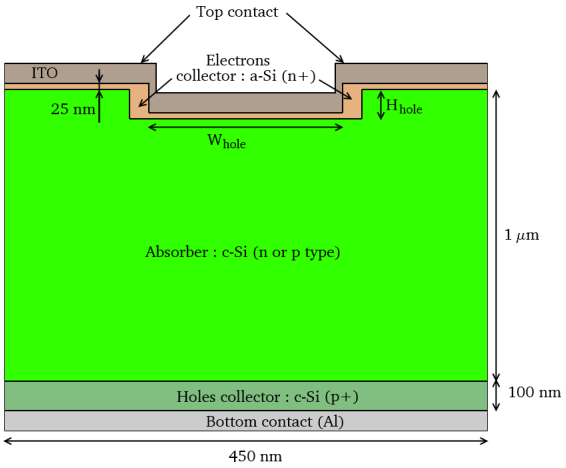

Figure 4: Slice view of the device (would correspond to the profiles in fig 2, with no through holes)

The amount of absorbed photons (N_{ph}^{abs}) in each domain of this thin film solar cell is depicted in figure 5. This later shows that low energy photons are mainly absorbed in the backside metal layer, demonstrating that an optical spacer may be useful.

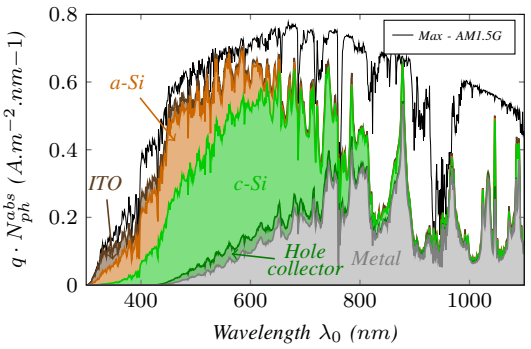

Figure 5: Amount of absorbed photons in each part of the device for the optimized design (3D-FDTD)

For an IQE equal to 1, the integration of the spectrum obtained in fig 5 leads to a current density between 12.8 $mA.cm^{-2}$ and 17.1 $mA.cm^{-2}$ depending on the carrier collection in the amorphous silicon (orange area).

2. ELECTRICAL SIMULATIONS

2.1. Description of the electrical structure

In this part, we use Silvaco to study different structures corresponding to the slice view refereed in fig 4.

The electrical properties that we consider are restricted to the available technological processes [9]. We will assume that the absorber ($3 \times 10^{16} cm^{-3}$, 1 μm thick) of the device will be obtained by epitaxy, and will be bonded onto a substrate (glass or silicon) thanks to an Aluminum layer which will also collect the photogenerated holes through a p doped layer. The top contact will be made of a n+ doped a-Si:H conformal deposit [10].

With such a process flow, the electrical junction can be located either on the pattern side (p type absorber) or on the backside (n type absorber). Last, the ITO layer is not taken into account for the following simulations

since the simulated device is very small and the doping of the electrons collector (a-Si) is high enough to hide the influence of this low resistive layer.

2.2. Simplifications of the electrical model

As the photogeneration rate $G_i(x, y, z)$ distribution is difficult to obtain when using a PC (we need to sum up all the contribution of each wavelength, and each FDTD simulation lasts many hours) we decide to simplify our analysis to obtain relevant results without loosing time waiting the FDTD results. For this reason, we artificially introduce a constant value of G_i that corresponds to a given optical power (i.e. 1 sun for instance). Full electro-optical optimizations using 3D FDTD maps to calculate G_i will be done in a future work.

The default values used for the following electrical simulations are sum up in table I.

Table I: non optimized parameters of the electrical simulations.

Parameter	Value
Equivalent optical power (sun)	1
Hole width (nm)	200
Hole height (nm)	100
n+ doping (cm^{-3})	10^{19}
Absorber doping (cm^{-3})	3×10^{16}
p+ doping (cm^{-3})	10^{18}

2.3. Influence of the sidewalls conductivity

In order to study the influence of the sidewalls conduction, we simulate both the device depicted in fig 4 and a variation for which the a-Si layer is not present on the vertical edges of the hole, to simulate an electrical discontinuity between the electrodes (on the surface) and the bottom of the holes. In this case, surface recombinations are located on the air-absorber interface on the vertical edges of the holes.

Figure 6 shows the relative influence of the surface recombinations on top and bottom side of the absorber for different configurations. For surface recombinations on the bottom interface (blue curves), the comparison between curves with full lines or dashed ones shows that electrical defects on the top surface has no influence, but selecting a n type absorber (bottom junction) results in a more robust solution.

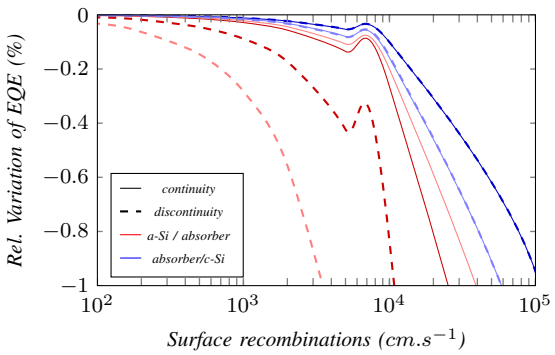

Figure 6: EQE variation (light colors stand for a p type absorber and dark curves correspond to a n type absorber)

Concerning the top surface (red curves), when the bottom part of the patterns is connected to the top surface (red full lines), the location of the junction has almost no influence. On the contrary, electrical discontinuities strongly degrade the efficiency of the device, but the n type absorber is once again less sensitive to these defaults.

For this last particular case, the electric simulation shows no electric field close to the sidewalls (fig. 7), but for the p type absorber, the electric field of the junction attracts carriers to the bottom part of the holes. These later must travel close to the sidewalls and recombine due to surface recombinations before reaching the top electrode. When the junction is on the backside, the device is less sensitive to low surface recombinations on the pattern.

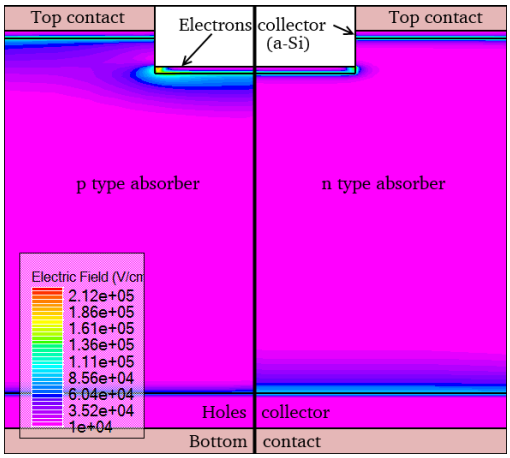

Figure 7: Map of the electrical field at maximum efficiency for a variation of the structure presented in figure 4 where no a-Si covers the sidewalls of the patterns (ITO has been replaced by a metal electrode).

2.4. Patterning holes at the end of the process flow

Another solution to pattern a thin film solar cell consists in fabricating the electrical junction (the collectors and the absorber), and then pattern the front surface and passivate the holes using a low index insulator (like silica or silicon nitride). Surface recombination are located on the interface between the air and the absorber or the absorber and a-Si, like in the previous part.

Contrary to the previous part, the bottom interface between the holes collector and the absorber behaves slightly differently from the reference with a top junction (blue curves in fig. 8): this particular device becomes the most sensitive device to the backside recombinations (with $S > 10^4\, cm.s^{-1}$). Moreover, such a device (dashed curves) is even more sensitive to surface combinations on the front side (red curves in fig. 7), compared to a non conformal layer (fig. 6).

This trend is mainly due to the surface increase where recombinations occur and no electrical field (fig. 9) drains the photogenerated carriers to the electrodes.

CONCLUSION

To achieve a robust and efficient solar cell, the optical optimization consists in achieveing a high photogeneration located in the absorber and far from the electrons

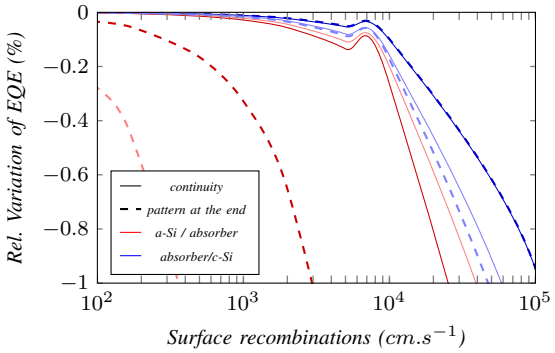

Figure 8: EQE variation (light colors stand for a p type absorber and dark curves correspond to a n type absorber)

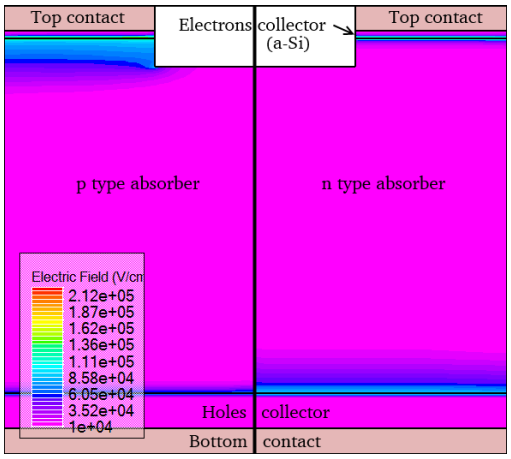

Figure 9: Map of the electrical field at maximum efficiency for a variation of the structure presented in figure 4 where the pattern would be fabricated after a-Si deposit (ITO has been replaced by a metal electrode).

or holes collectors. For thin film solar cells, it has been already demonstrated that using a 2D PC structure on the front side is an efficient way to increase the amount of absorbed photons in the active material. Apparently, the channeled light in the blue domain may generate carriers further from the top surface, where electrical collection can be efficient. For these particular wavelengths, work is still under process.

In the electric domain, we demonstrate that the most robust solution consists in a top collector that collects carriers on every sides of the pattern. A particular attention should be focused on the continuity of the contact on sidewalls of the pattern, since defaults may increase the sensitivity to surface passivation. Last, the most robust solution consists in locating the junction far from the patterned surface.

This work is supported by ANR (Nathisol Program) and FP7 program (PhotoNvoltaics, grant n^{o}309127).

REFERENCES

[1] B. Janthong, Y. Moriya, A. Hongsingthong, P. Sichanugrist, and M. Konagai, "Management of light-trapping effect for a-si: H/μc-si: H tandem solar cells using novel substrates, based on mocvd zno and etched white glass," *Solar Energy Materials and Solar Cells*, 2013.

[2] G. Demésy and S. John, "Solar energy trapping with modulated silicon nanowire photonic crystals," *Journal of Applied Physics*, vol. 112, no. 7, pp. 074 326–074 326, 2012.

[3] X. Meng, V. Depauw, G. Gomard, O. El Daif, C. Trompoukis, E. Drouard, C. Jamois, A. Fave, F. Dross, I. Gordon *et al.*, "Design, fabrication and optical characterization of photonic crystal assisted thin film monocrystalline-silicon solar cells," *Optics Express*, vol. 20, no. 104, pp. A465–A475, 2012.

[4] M. Zeman, O. Isabella, S. Solntsev, and K. Jäger, "Modelling of thin-film silicon solar cells," *Solar Energy Materials and Solar Cells*, 2013.

[5] M. G. Deceglie, V. E. Ferry, A. P. Alivisatos, and H. A. Atwater, "Design of nanostructured solar cells using coupled optical and electrical modeling," *Nano letters*, vol. 12, no. 6, pp. 2894–2900, 2012.

[6] G. Gomard, R. Peretti, E. Drouard, X. Meng, and C. Seassal, "Photonic crystals and optical mode engineering for thin film photovoltaics," *Optics Express*, vol. 21, no. 103, pp. A515–A527, 2013.

[7] W. Favre, J. Coignus, N. Nguyen, R. Lachaume, R. Cabal, and D. Munoz, "Influence of the transparent conductive oxide layer deposition step on electrical properties of silicon heterojunction solar cells," *Applied Physics Letters*, vol. 102, no. 18, pp. 181 118–181 118, 2013.

[8] V. Depauw, X. Meng, O. El Daif, G. Gomard, L. Lalouat, E. Drouard, C. Trompoukis, A. Fave, and I. Gordon, "Micron-thin crystalline-silicon solar cells integrating numerically optimized 2d photonic crystals," *Applied Physic letters*, Accepted.

[9] V. Depauw, Y. Qiu, K. Van Nieuwenhuysen, I. Gordon, and J. Poortmans, "Epitaxy-free monocrystalline silicon thin film: first steps beyond proof-of-concept solar cells," *Progress in Photovoltaics: Research and Applications*, vol. 19, no. 7, pp. 844–850, 2011.

[10] X. Wen, X. Zeng, W. Liao, Q. Lei, and S. Yin, "An approach for improving the carriers transport properties of a-si: H/c-si heterojunction solar cells with efficiency of more than 27%," *Solar Energy*, vol. 96, pp. 168–176, 2013.